

LETTER • OPEN ACCESS

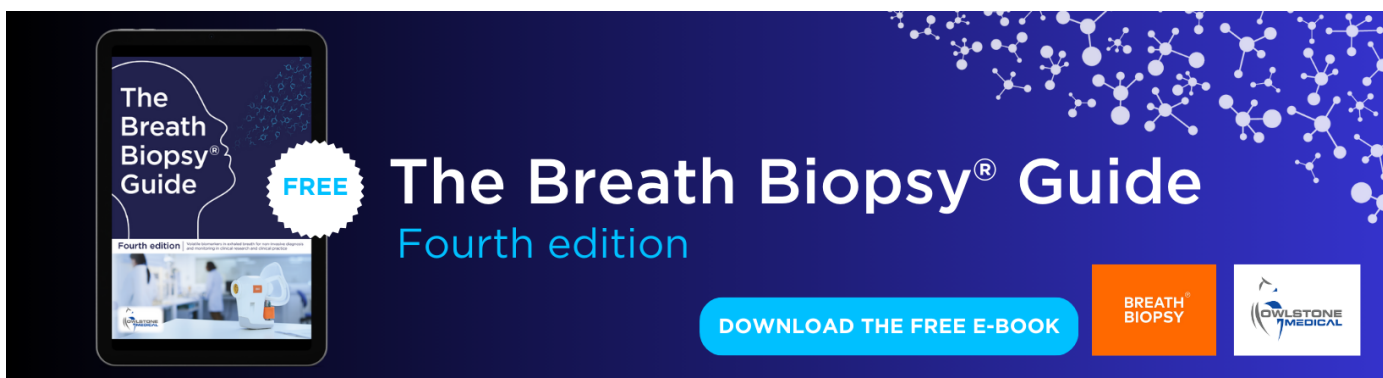
Impact of aerosol–meteorology interactions on fine particle pollution during China’s severe haze episode in January 2013

To cite this article: Jiandong Wang *et al* 2014 *Environ. Res. Lett.* **9** 094002

View the [article online](#) for updates and enhancements.

You may also like

- [Changing PM_{2.5} and related meteorology over India from 1950–2014: a new perspective from a chemistry-climate model ensemble](#)
Sarah Hancock, Arlene M Fiore, Daniel M Westervelt *et al.*
- [Outside in: the relationship between indoor and outdoor particulate air quality during wildfire smoke events in western US cities](#)
Katelyn O'Dell, Bonne Ford, Jesse Burkhardt *et al.*
- [Addressing the source contribution of PM_{2.5} on mortality: an evaluation study of its impacts on excess mortality in China](#)
Lin Tian, Qiang Zeng, Wentan Dong *et al.*



The Breath Biopsy® Guide
Fourth edition

FREE

DOWNLOAD THE FREE E-BOOK

BREATH BIOPSY

OWLSTONE MEDICAL

Impact of aerosol–meteorology interactions on fine particle pollution during China’s severe haze episode in January 2013

Jiandong Wang^{1,2}, Shuxiao Wang^{1,2}, Jingkun Jiang^{1,2}, Aijun Ding³, Mei Zheng⁴, Bin Zhao^{1,2}, David C Wong⁵, Wei Zhou^{1,2}, Guangjie Zheng^{1,2}, Long Wang^{1,2}, Jonathan E Pleim⁵ and Jiming Hao^{1,2}

¹ State Key Joint Laboratory of Environment Simulation and Pollution Control, School of Environment, Tsinghua University, Beijing, 100084, People’s Republic of China

² State Environmental Protection Key Laboratory of Sources and Control of Air Pollution Complex, Beijing 100084, People’s Republic of China

³ Institute for Climate and Global Change Research & School of Atmospheric Sciences, Nanjing University, Nanjing, People’s Republic of China

⁴ School of Environmental Science and Engineering, Peking University, Beijing, 100084, People’s Republic of China

⁵ US Environmental Protection Agency, Research Triangle Park, NC, USA

E-mail: shxwang@tsinghua.edu.cn

Received 10 May 2014, revised 21 July 2014

Accepted for publication 4 August 2014

Published 9 September 2014

Abstract

In January 2013, a severe regional haze occurred over the North China Plain. An online-coupled meteorology-chemistry model was employed to simulate the impacts of aerosol–meteorology interactions on fine particles (PM_{2.5}) pollution during this haze episode. The response of PM_{2.5} to meteorology change constituted a feedback loop whereby planetary boundary layer (PBL) dynamics amplified the initial perturbation of PM_{2.5}. High PM_{2.5} concentrations caused a decrease of surface solar radiation. The maximal decrease in daily average solar radiation reached 53% in Beijing, thereby leading to a more stable PBL. The peak PBL height in Beijing decreased from 690 m to 590 m when the aerosol extinction was considered. Enhanced PBL stability suppressed the dispersion of air pollutants, and resulted in higher PM_{2.5} concentrations. The maximal increase of PM_{2.5} concentrations reached 140 $\mu\text{g m}^{-3}$ in Beijing. During most PM_{2.5} episodes, primary and secondary particles increased simultaneously. These results imply that the aerosol–radiation interactions played an important role in the haze episode in January 2013.

 Online supplementary data available from stacks.iop.org/ERL/9/094002/mmedia

Keywords: meteorology, fine particles, aerosol–radiation interactions, haze, solar radiation

1. Introduction

While aerosol–radiation interactions (ARI) are clearly very important in the context of climate change Boucher *et al*

(2013), they also can have profound impacts on atmospheric chemistry and meteorology on short time scales in areas with high aerosol loading. Radiation scattering and absorption by atmospheric aerosols directly affect surface and air temperature along with semi-direct effects or rapid adjustments such as changes in atmospheric stability and cloud cover. Thus, consideration of ARI is not only important for climate models but also for numerical weather prediction and air quality models.



Content from this work may be used under the terms of the Creative Commons Attribution 3.0 licence. Any further distribution of this work must maintain attribution to the author(s) and the title of the work, journal citation and DOI.

To assess ARI, several online-coupled meteorology and chemistry models have been developed and applied (e.g. Jacobson 1994, Jacobson *et al* 1996, Jacobson 1997a, 1997b, Grell *et al* 2005, Wong *et al* 2012). Their development and applications have been reviewed by Zhang (2008), Grell and Baklanov (2011), Kukkonen *et al* (2012), Lee and Ngan (2011), Zhang *et al* (2012), El-Harbawi (2013), and Baklanov *et al* (2014). The impacts of aerosols on surface solar radiation, temperature profile, planetary boundary layer (PBL) stability, moisture, winds and precipitation have been analyzed using online models (Zhang *et al* 2007, Zhang *et al* 2010, Fan *et al* 2012). However, most of these studies focused on the change of meteorological parameters, but rarely mention that this modification of meteorology further increases the concentration of fine particulate matter with aerodynamic diameter equal to or less than $2.5\ \mu\text{m}$ ($\text{PM}_{2.5}$).

The rapid response of meteorology and air quality to aerosol effects during wildfires has been examined (Grell *et al* 2011, Fu *et al* 2012, Jiang *et al* 2012, Wong *et al* 2012). It has been reported that high aerosol concentrations would cool the surface, heat the atmosphere, increase the boundary layer stability, and suppress the dispersion of $\text{PM}_{2.5}$ (Andreae *et al* 2004, Koren *et al* 2004, Feingold *et al* 2005, Grell *et al* 2011, Wong *et al* 2012, Ding *et al* 2013). Some studies have reported the delay or reduction of precipitation by changing cloud process (Andreae *et al* 2004, Koren *et al* 2004, Feingold *et al* 2005, Tosca *et al* 2010, Grell *et al* 2011, Ding *et al* 2013). Reduction of O_3 due to the reduction of solar radiation was also reported (Jiang *et al* 2012, Wong *et al* 2012). In China, $\text{PM}_{2.5}$ concentrations during haze episodes could reach similar levels or even higher than those during wild fire episodes (Li *et al* 2013, Liu *et al* 2013, Zhang *et al* 2013), and haze episodes show different characteristics. First, the ratio of light-absorbing carbon in $\text{PM}_{2.5}$ is lower than that during wild fires (Andreae *et al* 2004, Feingold *et al* 2005, Grell *et al* 2011, Jiang *et al* 2012, Ding *et al* 2013). Second, the wild fire itself may cause perturbations in the meteorological system because of the additional heat release. Therefore, aerosol effects during haze episodes could be strong and with different characteristics. Studies on aerosol effects during haze episodes are quite limited (Quan *et al* 2013, Wang *et al* 2014).

In January 2013, a severe regional haze episode with daily $\text{PM}_{2.5}$ exceeding $500\ \mu\text{g m}^{-3}$ occurred over the North China Plain, which offered an opportunity to investigate the aerosol effects on meteorology and air quality. In this study, the two-way coupled WRF and Community Multi-scale Air Quality Model (CMAQ) system (WRF-CMAQ) was employed to explore the interactions between aerosols and meteorology and resulting effects on air pollutant concentrations during this severe winter haze episode. This study quantifies the feedback loop between $\text{PM}_{2.5}$ and meteorology, which can narrow the gap between models and observations of air pollution in January 2013, and thus helps improve our understanding of winter haze episodes.

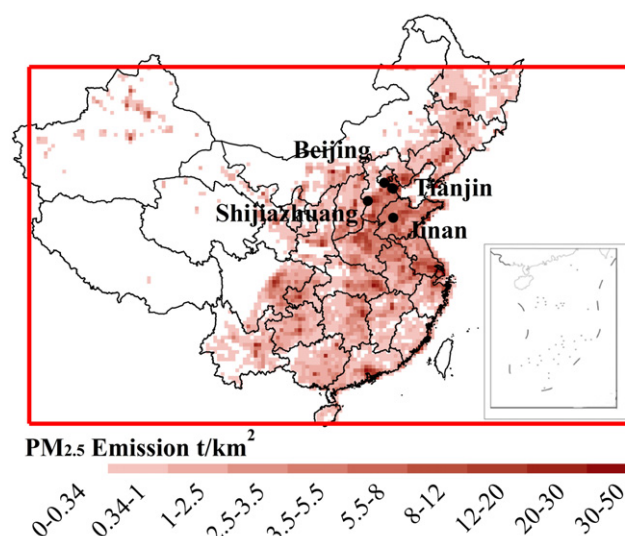


Figure 1. CMAQ modeling domain at a horizontal grid cell resolution of 36 km over China. The red frame shows the modeling domain and the black dots show the cities selected in this study. The colors show the emission intensity of $\text{PM}_{2.5}$.

2. Model configuration and observational data sources

2.1. Model configuration

The two-way coupled WRF-CMAQ system consists of three components: WRF version 3.4 developed by US National Center for Atmospheric Research, CMAQ version 5.0 developed by US Environmental Protection Agency and an inter-model coupler. Detailed information about the two-way coupled WRF-CMAQ system can be found in Wong *et al* (2012). The WRF model configuration include the WRF single-moment 6-class microphysics scheme (Hong and Lim 2006), version 2 of the Kain-Fritsch cumulus cloud parameterization (Kain 2004), the Asymmetric Convective Model version 2 for the PBL (Pleim 2007a, 2007b), the RRTMG radiation mechanism and the Pleim–Xiu land-surface model (Pleim and Xiu 1995 and Xiu and Pleim 2001) with indirect soil moisture and temperature nudging (Pleim and Xiu 2003, Pleim and Gilliam 2009). The CMAQ model is configured using the AERO6 aerosol module and the CB05 gas-phase chemical mechanism. Although interactions between particulate matter and meteorology include ARI and aerosol–cloud interaction, only ARI is considered in this study.

The modeling domain, as shown in figure 1, covers most of China and part of East Asia with $36\ \text{km} \times 36\ \text{km}$ grid resolutions. Both WRF and CMAQ use 23 vertical layers. The model simulation period is from 1 to 31 January 2013. The configurations of chemical initial conditions and boundary conditions, domain configuration, and emission inventory are consistent with our previous papers (Zhao *et al* 2013a, 2013b). In order to quantify the ARI, two scenarios, with shortwave feedback (SF) and without feedback (NF) are simulated.

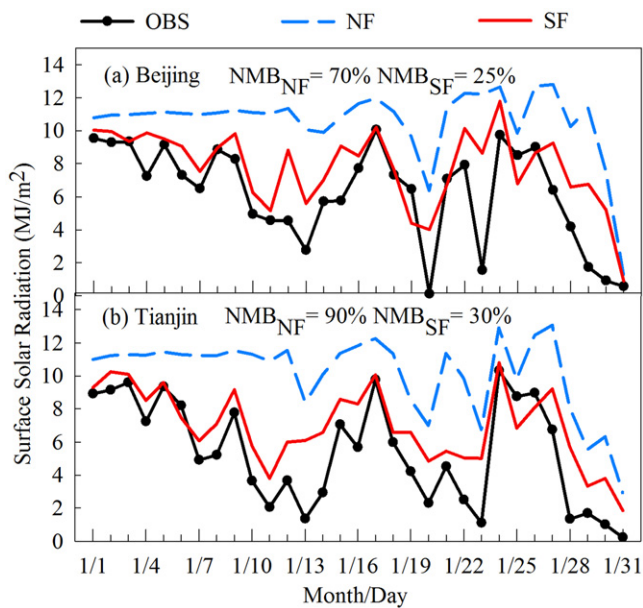


Figure 2. Simulated and observed surface solar radiation data for Beijing (a) and Tianjin (b), in January 2013. The black line with dots, blue dashed line and the red solid line show the observed solar radiation, simulated surface solar radiation in NF scenario and simulated surface solar radiation SF scenario, respectively.

2.2. Observational data sources

Observed PM_{2.5} hourly mass concentrations at Tianjin, Shijiazhuang and Jinan in the North China Plain are obtained from China National Urban Air Quality Real-time Publishing Platform (<http://113.108.142.147:20035/emcpublish/>). For a given city, PM_{2.5} hourly mass concentration is represented by the average of data from all monitoring sites located in the city. Since the PM_{2.5} data in Beijing are not included in this platform until January 17th, the observed data from State Key Joint Laboratory of Environmental Simulation and Pollution Control, Peking University is used instead. The locations of those cities are shown in figure 1. Daily total solar radiation observation data at Beijing and Tianjin are downloaded from China Meteorological Data Sharing Service System (<http://cdc.cma.gov.cn/>). The observed PBL height data is limited in China, therefore, PBL heights obtained from the Global Data Assimilation System (GDAS) (Rolph 2013) are used. GDAS is assimilated by surface observations, balloon data, wind profiler data, aircraft reports, buoy observations, radar observations, and satellite observations. It includes analyses at 00:00, 06:00, 12:00, and 18:00UTC and forecast fields at three hours after each analysis. The UTC time is converted to China Standard Time by adding 8 h to Beijing Time in China.

3. Results and discussion

3.1. Impact of feedback on meteorology

3.1.1. Impact of feedback on surface solar radiation. The simulated and observed surface solar radiation data at Beijing and Tianjin are shown in figures 2(a) and (b), respectively.

The simulated and observed daily total solar radiation were calculated by integrating the hourly surface solar irradiance from 0:00 to 23:59. At the Beijing site, the correlation coefficient (R) of simulated surface solar radiation for NF scenario and observed surface solar radiation is 0.35. The normalized mean bias (NMB) is 0.70. For SF scenario, R is 0.55 and NMB is 0.25, shown in table 1. At the Tianjin site, R of simulated surface solar radiation for NF scenario and observed surface solar radiation is 0.55. The NMB is 0.90. For SF scenario, R is 0.82 and NMB is 0.3. These results indicate that the model with aerosol feedbacks better captured the trend and magnitude of surface solar radiation.

The difference between surface solar radiations of NF and SF scenarios is due to the column accumulation of aerosol extinction. The simulated daily average reduction of total surface solar radiation in January was 2.8 MJ m⁻² and 3.2 MJ m⁻² for Beijing and Tianjin, respectively, which translates into 26% and 31% reduction of surface solar radiation. Detailed statistical information is shown in table 1. The maximal reduction for Beijing and Tianjin occurred on 10, 11 and 19 January, consistent with periods when high PM_{2.5} concentration were recorded (figure 4). The maximal reduction reached 5.9 and 7.1 MJ m⁻² for Beijing and Tianjin, respectively, representing 53% and 65% of daily solar radiation in NF scenario, a dramatic modification of surface solar radiation. Solar radiation absorbed by the surface of the Earth, heats the bottom of the atmospheric column producing convective eddies that transport heat and water vapor upward driving the growth of the PBL (Lee and Ngan 2011). The decrease of solar radiation leads to a decrease daytime PBL height.

3.1.2. Impact of feedback on PBL height. Simulated and GDAS diurnal average PBL heights for Beijing are shown in figure 3. NMB for simulated PBL height of NF scenario compared to GDAS was 0.2. With SF scenario, the NMB decreased to -0.04. The aerosol extinction affects the PBL temperature in two ways, as shown in figure S1. On the surface, it causes a decrease of surface solar radiation, which leads to a decrease of surface temperature. Meanwhile, the absorption of light-absorbing particles such as black carbon (BC) increases the temperature of the upper PBL. This process enhances the temperature inversion during the haze episode and leads to a more stable PBL. During the daytime, PBL height of the NF scenario is higher than the SF scenario. Peak PBL height of the NF simulation is 690 m but the SF scenario is only 590 m. The lower PBL height suppresses vertical mixing and dispersion of the pollutants, which in turn results in higher concentrations.

3.1.3. Impact of feedback on temperature, wind speed and humidity. The daily average temperature, wind speed, and humidity of east China in January 2013 are given in figures S2–S4. For a wide range of spatial and temporal scale, such as east China, the surface temperature decreases due to the reduced surface solar radiation, which is caused by aerosol extinction. The wind speed is slightly decreased, due to the

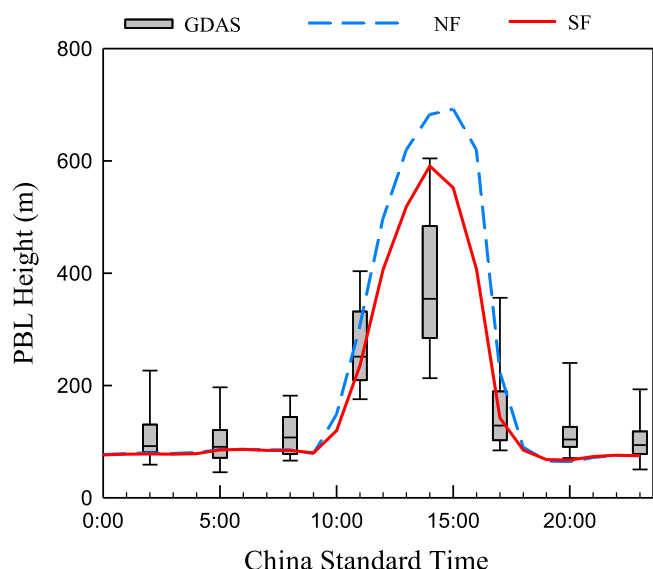


Figure 3. Simulated and assimilated diurnal average PBL height in Beijing, January 2013. The blue dashed line and the red solid line show the PBL heights of NF and SF scenario, respectively. The gray box shows the GDAS data. The central rectangle spans the first quartile to the third quartile. The segment inside the rectangle shows the median. The whiskers above and below the box are the 5th and 95th percentiles. According to the Sunrise and sunset time in Beijing in January 8:00–17:00 is defined as daytime and the other is defined as nighttime.

reduction of driving force and more stable PBL. The decreased wind speed also suppressed the dispersion of pollutants. However, no significant differences were observed on humidity between NF and SF scenarios for east China.

3.2. Impact of feedback on PM_{2.5} pollution

Figure 4 shows the simulated and observed hourly average PM_{2.5} mass concentrations in January 2013. NMB of PM_{2.5} mass concentrations for the NF scenario is -0.19, -0.34, -0.28 and -0.27 for Beijing, Shijiazhuang, Tianjin and Jinan, respectively. Simulations of NF scenario matched well with the observations when PM_{2.5} concentrations were low. However, during heavily polluted periods, the simulated PM_{2.5} in the NF scenario is significantly underestimated. For the hours when observed data were over 300 μg m⁻³, the PM_{2.5} in NF scenario showed 40%, 46%, 22% and 46%

underestimation for Beijing, Shijiazhuang, Tianjin and Jinan, respectively.

Considering the aerosol feedback, the NMB of simulated PM_{2.5} mass concentrations for the SF scenario are -0.03, -0.24, -0.19 and -0.16 for Beijing, Shijiazhuang, Tianjin and Jinan, respectively. Although PM_{2.5} concentration in the SF scenario was still underestimated due to uncertainties in secondary organic aerosol mechanism in CMAQ Baek *et al* (2011), the model performance was largely improved. Taking Beijing as an example (figure 4(b)), PM_{2.5} mass concentrations in both NF and SF scenarios are similar during low concentration periods. For heavily polluted periods (9–11th, 18–19th and 28–30th), however, the PM_{2.5} mass concentrations in the SF scenario are much higher than those in the NF scenario and closer to the observed data. The difference of PM_{2.5} mass concentrations between the NF and SF scenarios gets larger as the PM_{2.5} pollution gets worse. For the hours when observed data were greater than 300, the PM_{2.5} in SF scenario showed 23%, 37%, 10% and 36% underestimation for Beijing, Shijiazhuang, Tianjin and Jinan, respectively. The maximal increase of PM_{2.5} in the SF scenario over the NF scenario is 140 μg m⁻³ during the simulation period. The data for other cities have similar trends, implying that the aerosol feedback should not be neglected when modeling severe haze episodes.

Figure 5 shows the difference of hourly average PM_{2.5} species mass concentrations between SF and NF scenarios for Beijing from 12 January to 24 January 2013. The average increases of PM_{2.5} mass concentration from NF to SF scenario are 6.2, 2.3, 5.5, 2.7, 8.1, and 14.0 μg m⁻³ for NO₃⁻, SO₄²⁻, NH₄⁺, EC, OC and other species, respectively. Compared with NF scenario, NO₃⁻, SO₄²⁻, NH₄⁺, EC, OC and other species grew 20.4%, 15.2%, 18.5%, 30.3%, 30.2% and 33.5%, respectively. The increase for Shijiazhuang, Tianjin and Jinan is shown in table S1. It was found that primary particles (EC, part of OC and others) and secondary particles (NO₃⁻, SO₄²⁻, NH₄⁺ and part of OC, the secondary OC is rather small compared with primary OC in simulation) increased simultaneously. However the ratio of primary particles increase was larger than that of secondary particles, which implied that the growth mechanism of primary and secondary PM_{2.5} mass concentration were not identical. The vertical mixing of air pollutants was suppressed due to the lower PBL height (as discussed in section 3.2), which caused the increase of both

Table 1. Observed and modeled average surface solar radiation, PBL height, and PM_{2.5} in Beijing, Tianjin, Shijiazhuang and Jinan in January 2013.

Variable	City	OBS	NF	SF	NMB _{NF}	NMB _{SF}	(SF-NF)/NF(%)
Surface solar radiation (MJ m ⁻²)	Beijing	6.23	10.61	7.81	0.70	0.25	-26.39
	Tianjin	5.36	10.17	6.97	0.90	0.30	-31.47
PBL height (m)	Beijing		692.71	552.37			-20.26
PM _{2.5} mass concentration (μg m ⁻³)	Beijing	148.30	119.87	143.66	-0.19	-0.03	19.85
	Shijiazhuang	300.09	197.88	227.11	-0.34	-0.24	14.77
	Tianjin	155.91	112.18	125.52	-0.28	-0.19	11.89
	Jinan	227.13	166.58	190.88	-0.27	-0.16	14.58

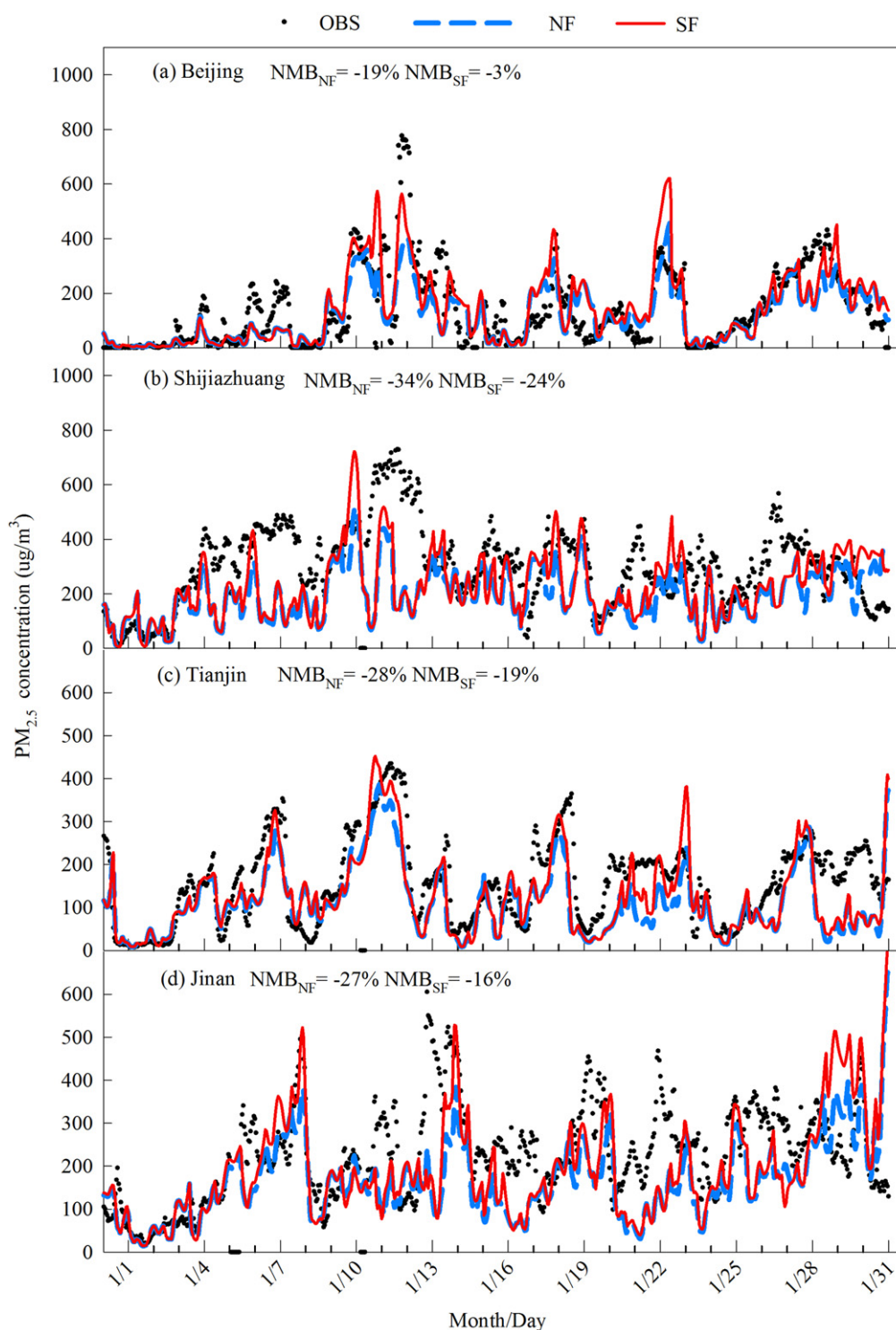


Figure 4. Hourly average $PM_{2.5}$ mass concentrations for Beijing (a), Tianjin (b), Shijiazhuang (c) and Jinan (d) in January 2013. The black dots, blue dashed line and the red solid line show the observed $PM_{2.5}$ concentrations, $PM_{2.5}$ simulations in NF scenario and $PM_{2.5}$ simulations in SF scenario, respectively.

primary and secondary particle levels. The decrease of PBL height and wind should have similar impact on primary and secondary $PM_{2.5}$. However, the mechanism for secondary $PM_{2.5}$ increase was more complicated. Figure S5 shows that the ozone concentration is reduced in most places of China. The ozone reduction region is consistent with the solar

reduction region and the free radicals reduction region. It indicates that the reduction of solar radiation leads to a decrease of photo-reaction rate. The formation of free radicals is suppressed and atmospheric oxidation is reduced. The reduced atmospheric oxidation decreases the formation of secondary $PM_{2.5}$. On the other hand, decreased surface

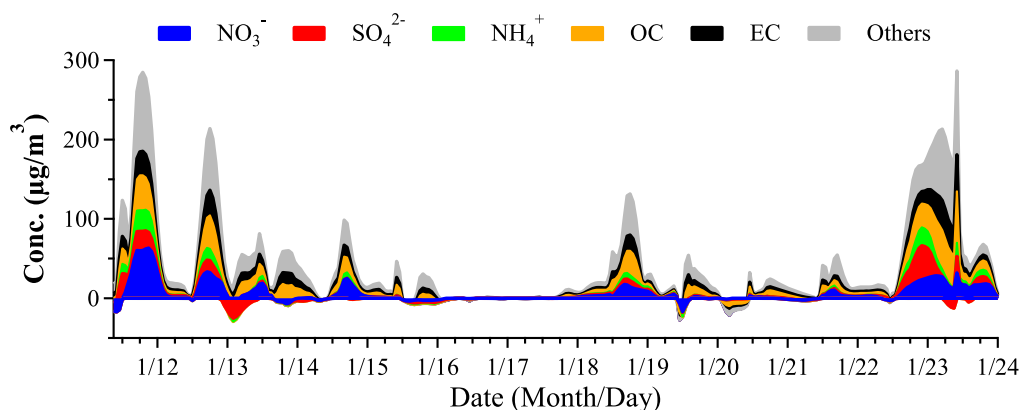


Figure 5. Difference of hourly average $PM_{2.5}$ species between SF and NF scenario (SF-NF) for Beijing from 12 January to 24 January 2013. The blue, red, green, yellow, black, and gray area show the difference of nitrate (NO_3^-), sulfate (SO_4^{2-}), ammonia (NH_4^+), organic carbon (OC), elemental carbon (EC), and other species mass concentration between SF and NF scenario, respectively.

temperature, shown in figure S1, also decrease the rate atmospheric aerosol formation reaction. The dispersion suppression and reduction of formation rate lead to a smaller growth ratio of secondary particles.

4. Conclusion

This study demonstrates the feedback loop during haze episodes whereby aerosols affect meteorology through changes in radiation and PBL dynamics thereby increasing $PM_{2.5}$ concentrations. The high $PM_{2.5}$ levels affect the temperature of the PBL in two ways. At ground-level, $PM_{2.5}$ pollution causes a decrease of surface solar radiation, which leads to a decrease of surface temperature. Meanwhile, the absorption of light-absorbing particles such as BC increases the temperature of the upper PBL. This process enhances the temperature inversion during the haze episode, leading to a more stable PBL. Enhanced PBL stability initiated by aerosols suppresses the vertical mixing and dispersion of the air pollutants, resulting in higher $PM_{2.5}$ concentrations. These results imply that the aerosol feedback shall not be neglected when simulating heavy haze episodes. Considering such feedback loop helps bridge the gap between model simulations and observations.

Due to the feedback loop, the initial perturbation due to emissions could be amplified. Emissions of $PM_{2.5}$ and its precursors could enhance the adverse meteorological conditions for dispersion of pollutants and finally result in extremely high pollution events. This implies that ARI play an important role in understanding the evolution of the winter haze episodes in China. Additionally, during haze episodes, emission reduction measures may be particularly effective.

Acknowledgments

This work was sponsored by National Natural Science Foundation of China (21221004), MEP's Special Funds for

Research on Public Welfares (201309009 and 201409002), Strategic Priority Research Program of the Chinese Academy of Sciences (XBD05020300) and special fund of State Key Joint Laboratory of Environment Simulation and Pollution Control (12L05ESPC). The authors also appreciate the support from the Collaborative Innovation Center for Regional Environmental Quality and support from Prof Michael B McElroy and Mr Chris Nielsen of China Project, School of Engineering and Applied Science, Harvard University. We thank Weidong Guo, Scott Voorhees, and Xueying Zhang for their helpful discussion.

References

- Andreae M O, Rosenfeld D, Artaxo P, Costa A A, Frank G P, Longo K M and Silva-Dias M A F 2004 Smoking rain clouds over the amazon *Science* **303** 1337–42
- Baek J, Hu Y, Odman M T and Russell A G 2011 Modeling secondary organic aerosol in CMAQ using multigenerational oxidation of semi-volatile organic compounds *J. Geophys. Res.* **116** D22204
- Baklanov A *et al* 2014 Online coupled regional meteorology chemistry models in Europe: current status and prospects *Atmos. Chem. Phys.* **14** 317–98
- Boucher O *et al* 2013 Clouds and aerosols *Climate Change 2013: The Physical Science Basis. Contribution of Working Group I to the Fifth Assessment Report of the Intergovernmental Panel on Climate Change* ed T F Stocker, D Qin, G-K Plattner, M Tignor, S K Allen, J Boschung, A Nauels, Y Xia, V Bex and P M Midgley (Cambridge: Cambridge University Press)
- Ding A J *et al* 2013 Intense atmospheric pollution modifies weather: a case of mixed biomass burning with fossil fuel combustion pollution in eastern China *Atmos. Chem. Phys.* **13** 10545–54
- El-Harabawi M 2013 Air quality modelling, simulation, and computational methods: a review *Environ. Rev.* **21** 149–79
- Fan J, Leung L R, Li Z, Morrison H, Chen H, Zhou Y, Qian Y and Wang Y 2012 Aerosol impacts on clouds and precipitation in eastern China: results from bin and bulk microphysics *J. Geophys. Res.* **117** D00K36
- Feingold G, Jiang H and Harrington J Y 2005 On smoke suppression of clouds in amazonia *Geophys. Res. Lett.* **32** L02804
- Fu J S, Hsu N C, Gao Y, Huang K, Li C, Lin N H and Tsay S C 2012 Evaluating the influences of biomass burning during

- 2006 BASE-ASIA: a regional chemical transport modeling *Atmos. Chem. Phys.* **12** 3837–55
- Grell G and Baklanov A 2011 Integrated modeling for forecasting weather and air quality: A call for fully coupled approaches *Atmos. Environ.* **45** 6845–51
- Grell G, Freitas S R, Stuefer M and Fast J 2011 Inclusion of biomass burning in WRF-Chem: impact of wildfires on weather forecasts *Atmos. Chem. Phys.* **11** 5289–303
- Grell G A, Peckham S E, Schmitz R, McKeen S A, Frost G, Skamarock W C and Eder B 2005 Fully coupled 'online' chemistry within the WRF model *Atmos. Environ.* **39** 6957–75
- Hong S-Y and Lim J-O J 2006 The WRF single-moment 6-class microphysics scheme (WSM6) *J. Korean Meteor. Soc.* **42** 129–51
- Jacobson M Z 1994 Developing, coupling, and applying a gas, aerosol *Transport, and Radiation Model to Study Urban and Regional Air Pollution* PhD Dissertation University of California, Los Angeles
- Jacobson M Z 1997a Development and application of a new air pollution modeling system: II. Aerosol module structure and design *Atmos. Environ.* **31** 131–44
- Jacobson M Z 1997b Development and application of a new air pollution modeling system: III. Aerosol-phase simulations *Atmos. Environ.* **31** 587–608
- Jacobson M Z, Lu R, Turco R P and Toon O B 1996 Development and application of a new air pollution modeling system: I. Gas-phase simulations *Atmos. Environ.* **30** 1939–63
- Jiang X Y, Wiedinmyer C and Carlton A G 2012 Aerosols from fires: an examination of the effects on ozone photochemistry in the western United States *Environ. Sci. Technol.* **46** 11878–86
- Kain J S 2004 The kain–fritsch convective parameterization: an update *J. Appl. Meteorol.* **43** 170–81
- Koren I, Kaufman Y J, Remer L A and Martins J V 2004 Measurement of the effect of amazon smoke on inhibition of cloud formation *Science* **303** 1342–5
- Kukkonen J et al 2012 A review of operational, regional-scale, chemical weather forecasting models in Europe *Atmos. Chem. Phys.* **12** 1–87
- Lee P and Ngan F 2011 Coupling of important physical processes in the planetary boundary layer between meteorological and chemistry models for regional to continental scale air quality forecasting: an overview *Atmosphere* **2** 464–83
- Li Z et al 2013 Aerosol physical and chemical properties retrieved from ground-based remote sensing measurements during heavy haze days in Beijing winter *Atmos. Chem. Phys.* **13** 10171–83
- Liu X G et al 2013 Formation and evolution mechanism of regional haze: a case study in the megacity Beijing, China *Atmos. Chem. Phys.* **13** 4501–14
- Pleim J E 2007a A Combined local and nonlocal closure model for the atmospheric boundary layer. part II: application and evaluation in a mesoscale meteorological model *J. Appl. Meteorol. Climatol.* **46** 1396–409
- Pleim J E 2007b A combined local and nonlocal closure model for the atmospheric boundary layer. part I: model description and testing *J. Appl. Meteorol. Climatol.* **46** 1383–95
- Pleim J E and Xiu A 1995 Development and testing of a surface flux and planetary boundary layer model for application in mesoscale models *J. Appl. Meteorol.* **34** 16–32
- Pleim J E and Xiu A 2003 Development of a land surface model. part II: data assimilation *J. Appl. Meteorol.* **42** 1811–22
- Pleim J E and Gilliam R 2009 An indirect data assimilation scheme for deep soil temperature in the Pleim–Xiu land surface model *J. Appl. Meteorol. Climatol.* **48** 1362–76
- Quan J, Gao Y, Zhang Q, Tie X, Cao J, Han S, Meng J, Chen P and Zhao D 2013 Evolution of planetary boundary layer under different weather conditions, and its impact on aerosol concentrations *Particuology* **11** 34–40
- Rolph G D 2013 *Real-Time Environmental Applications and Display System (READY)* (Silver Spring, MD: NOAA Air Resources Laboratory) (<http://ready.arl.noaa.gov>)
- Tosca M G, Randerson J T, Zender C S, Flanner M G and Rasch P J 2010 Do biomass burning aerosols intensify drought in equatorial Asia during El Niño? *Atmos. Chem. Phys.* **10** 3515–28
- Wang Z et al 2014 Modeling study of regional severe hazes over mid-eastern China in january 2013 and its implications on pollution prevention and control *Sci. China Earth Sci.* **57** 3–13
- Wong D C, Pleim J, Mathur R, Binkowski F, Otte T, Gilliam R, Pouliot G, Xiu A, Young J O and Kang D 2012 WRF-CMAQ two-way coupled system with aerosol feedback: software development and preliminary results *Geosci. Model Dev.* **5** 299–312
- Xiu A and Pleim J E 2001 Development of a land surface model. part I: application in a mesoscale meteorological model *J. Appl. Meteorol.* **40** 192–209
- Zhang R, Hegg D A, Huang J and Fu Q 2013 Source attribution of insoluble light-absorbing particles in seasonal snow across northern China *Atmos. Chem. Phys. Discuss.* **13** 6091–99
- Zhang R, Li G, Fan J, Wu D L and Molina M J 2007 Intek linked to Asian pollution *Proc. Natl. Acad. Sci.* **104** 5295–9
- Zhang Y 2008 Online-coupled meteorology and chemistry models: history, current status, and outlook *Atmos. Chem. Phys.* **8** 1833–912
- Zhang Y, Bocquet M, Mallet V, Seigneur C and Baklanov A 2012 Real-time air quality forecasting, part I: history, techniques, and current status *Atmos. Environ.* **60** 632–55
- Zhang Y, Wen X Y and Jang C J 2010 Simulating chemistry–aerosol–cloud–radiation–climate feedbacks over the continental US using the online-coupled weather research forecasting model with chemistry (WRF/chem) *Atmos. Environ.* **44** 3568–82
- Zhao B, Wang S X, Dong X Y, Wang J D, Duan L, Fu X, Hao J M and Fu J 2013a Environmental effects of the recent emission changes in China: implications for particulate matter pollution and soil acidification *Environ. Res. Lett.* **8** 024031
- Zhao B, Wang S, Wang J, Fu J S, Liu T, Xu J, Fu X and Hao J 2013b Impact of national NO_x and SO₂ control policies on particulate matter pollution in China *Atmos. Environ.* **77** 453–63